Suppression of superconductivity by the nonmagnetic ions Zn and Al for the $YBa_2Cu_3O_{7-\delta}$ system: From dopant clusters to carrier localization

Pinglin Li, Jincang Zhang,* Guixin Cao, Chao Jing, and Shixun Cao
Department of Physics, Shanghai University, Shanghai 200436, People's Republic of China
(Received 27 May 2003; revised manuscript received 13 October 2003; published 30 June 2004)

To clarify the suppressing mechanism of Zn and Al substitution on high-T_c superconductivity, positron annihilation experiment and simulated calculation are used to study systemically the $YBa_2Cu_{3-x}(Zn,Al)_xO_{7-\delta}$ ($x=0.0-0.4$) cuprates. The results show that Zn doping ions prefer to combine into the cluster of seven ions with a double square and Al doping ions prefer to form six-ion-cluster with a hexamer structure, respectively. These clusters, especially for Zn, would evidently influence the positron annihilation characteristics, which can be seen from the variation of n_e with Zn content x in the clustering process. n_e displays an abrupt change as the impurity phases appear in both Zn and Al doping systems. From the doping process, Zn ions occupy Cu(2) sites in the CuO_2 planes and make the change of electron structure, resulting in the carrier localization. As a result, it interferes the pairing and transportation of superconducting carriers and then suppresses the superconductivity with the formation of Zn clusters. While Al ions enter Cu(1) sites in the Cu-O chains, they induce the localization of hole carriers and weaken the function of carrier reservoir by forming clusters. Therefore, the carriers cannot easily transfer to the CuO_2 planes. Since Al doping does not affect the pairing and transportation directly, it suppresses the superconductivity weakly than Zn doping. The effect of pairing and transportation of carriers on charge transfer is also discussed.

DOI: 10.1103/PhysRevB.69.224517 PACS number(s): 74.72.Bk, 78.70.Bj

I. INTRODUCTION

In the cuprate superconductors, a $YBa_2Cu_3O_{7-\delta}$ (YBCO) system has the typical CuO_2 plane and the Cu-O chain structure, thus it is an ideal object in the basic research and attracts a lot of attention.[1,2] In order to clarify the physical mechanism of high T_c superconductivity, element substitution plays an important role in the investigation of cuprate superconductors.[3–6] As nonmagnetic ions, Zn and Al have different doping behaviors in YBCO systems, namely, Zn substituting for Cu(2)[7] while Al for Cu(1) sites.[8,9] According to the magnetic break-pair, both substitutions should not induce the effect of break-pair. Therefore they should be less prominent than magnetic ions to influence the superconductivity. However, experimental results violate the theoretic predictions. As bivalent ion, Zn doping suppresses forcefully the superconductivity, whereas Al as trivalent doped ions affects superconductivity less than Zn.[10,11] As far as both manners in influence on the superconductivity, most researchers believe the CuO_2 planes are places where the superconductivity occurs.[12–15] Once some doped ions enter the CuO_2 planes the superconductivity will be suppressed severely, such as Zn doping. While the Cu-O chains and other layers play the role of carrier reservoirs, which affects indirectly the superconductivity, thus little doped Al ions do not evidently influence on T_c, and for larger Al content, the superconductivity will be suppressed.

In order to understand the suppression mechanism on superconductivity by the nonmagnetic ions in different doping sites, we should distinguish the occupied sites, the distribution of doping ions, and the change of electron structures. As an effective probe to the microstructures, defects and phase transition, positron annihilation technique (PAT) plays an important role in the study on condensed matter, including semiconductor, metal, alloy, and high-T_c cuprates etc.[16–19] For high-T_c superconductors, there have been some positron studies to elucidate the properties of the normal and superconducting states, including the Fermi surface, O-T transition, electron structure, and the carrier distributions.[20–25] In the present work, we studied systematically $YBa_2Cu_3O_{7-\delta}$ with Al and Zn substitution by the PAT experiment and simulated calculation using Islam and Ananthamohan method.[26] The results indicate that doping Zn and Al ions may combine into two, four, six, or seven ions clusters. From probability, Zn prefer to gather into seven ions cluster with a double square structure and Al form six ions cluster with a hexamer structure. All of them cause the variation of electron structure and the carrier localization. The superconducting electron pairing and transportation are also affected in different manners and extents. These characteristics are consistent with the results of PAT experiments and the variation of superconductivity.

II. EXPERIMENT

The experimental samples with nominal composition of $YBa_2Cu_{3-x}M_xO_y$ (M=Zn, Al; $x=0-0.4$) were prepared by solid-state reactions from appropriate amounts of high purity Y_2O_3, $BaCO_3$, CuO, ZnO, and Al_2O_3. The starting materials were mixed, ground, and calcined first at 920°C for 12 h. Then, the obtained precursors were reground, pressed to pellets, and sintered at 920°C for 24 h followed by furnace cooling. The resistivity was measured by the standard dc four-probe method with the voltage resolution of 10^{-7} V (HP3457A). The structure of the samples were analyzed by the powder x-ray diffraction (XRD, Cu-K_α) using the *D/max-B* x-ray diffractometer. For the $YBa_2Cu_3O_{7-\delta}$ doping-free ($T_c=93.0$ K) and low doping sample, the XRD

TABLE I. Experimental results of positron annihilation parameters for Zn and Al doped $YBa_2Cu_3O_{7-\delta}$ systems.

Zn content	0.0	0.02	0.04	0.08	0.1	0.12	0.2	0.3	0.4
τ_1 (ps)	195±3.9	195±3.9	189±3.8	182±3.6	184±3.7	189±3.8	184±3.7	185±3.7	182±3.6
τ_2 (ps)	544±22	541±22	561±22	554±22	551±22	556±22	528±21	557±22	553±22
I_1 (%)	91.2±1.82	87.3±1.74	86.2±1.72	86.7±1.73	87.8±1.74	87.9±1.74	86.4±1.72	87.7±1.75	86.7±1.73
Al content	0.0	0.05		0.1	0.15	0.2		0.3	0.4
τ_1 (ps)	195±3.9	196±3.8		197±3.9	203±3.8	206±3.6		201±3.7	205±3.6
τ_2 (ps)	544±22	581±22		553±22	552±22	549±21		565±22	557±22
I_1 (%)	91.2±1.82	94.0±1.76		92.2±1.8	91.9±1.75	92.1±1.73		93.3±1.76	92.8±1.74

results show single Y123 orthorhombic structure. With the increasing of substitution content, few unidentified peaks appear with very weak intensity at $x \geqslant 0.12$ for Zn and $x \geqslant 0.20$ for Al, respectively. The positron lifetime spectra were measured at a constant temperature ($20 \pm 0.5\,^{\circ}C$) using the *ORTEC-100U* fast-fast coincidence lifetime spectrometer. Two pieces of identical samples were sandwiched together with a 10 μC ^{22}Na positron source deposited on a thin Mylar foil (about 1.2 mg/cm^2 thickness). Each spectrum contains more than 1×10^6 counts. After subtracting background and source contributions, the lifetime spectra were analyzed with two-lifetime components by the POSITRONFIT-EXTENDED program with the best fit ($\chi^2 \leqslant 1.2$). The positron lifetime spectra are measured at the same environmental temperature for all the samples and the results are repeatable. Table I lists the positron experimental results of Zn and Al doping systems.

III. RESULTS AND DISCUSSION

A. Effect of Zn and Al doping on structure and superconductivity

Figure 1 gives the change of lattice parameters with doping content x, which was calculated by the least-squares method from powder XRD data. From Fig. 1(a), it can be seen that the lattice parameter a and b increase slightly with the increase of Zn content x, but O-T transition does not occur in the whole doping range of $x=0-0.4$ while the O-T transition occurs near $x=0.15$ for Al doping. Generally, the O-T transition is induced from the oxygen content in the Cu-O chains. Thus the variation of lattice parameters a and b imply that Al doping ions enter mainly Cu(1) sites, which is consistent with the Hoffmann *et al.*[9] and the Bringley *et al.*[27] results. It should be noticed that the O-T transition occurs before the appearance of impurity phases, which reflects the intrinsic properties of Al doping Y123 systems. For the same reason, the results of lattice parameters show that Zn doping ions would mainly enter Cu(2) sites in the CuO_2 planes.[28–30] It is well known that the superconductivity occurs in the CuO_2 planes, which implies that the superconductivity suppressed by Zn doping should be stronger than Al doping. Figure 2 shows the variation of T_c as a function of Zn and Al content x. For the undoped Y123 compound, T_c is 93 K, and then T_c falls to 72.3 K for Zn content of $x=0.1$, while for $x=0.4$, T_c is only 15.7 K. In contrast, for Al substitution, the T_c changes slightly to 91.5 K at $x=0.1$, while for the maximum substitution $x=0.4$, T_c is still 42.5 K. Obviously, Zn substitution suppresses superconductivity much more than Al does.

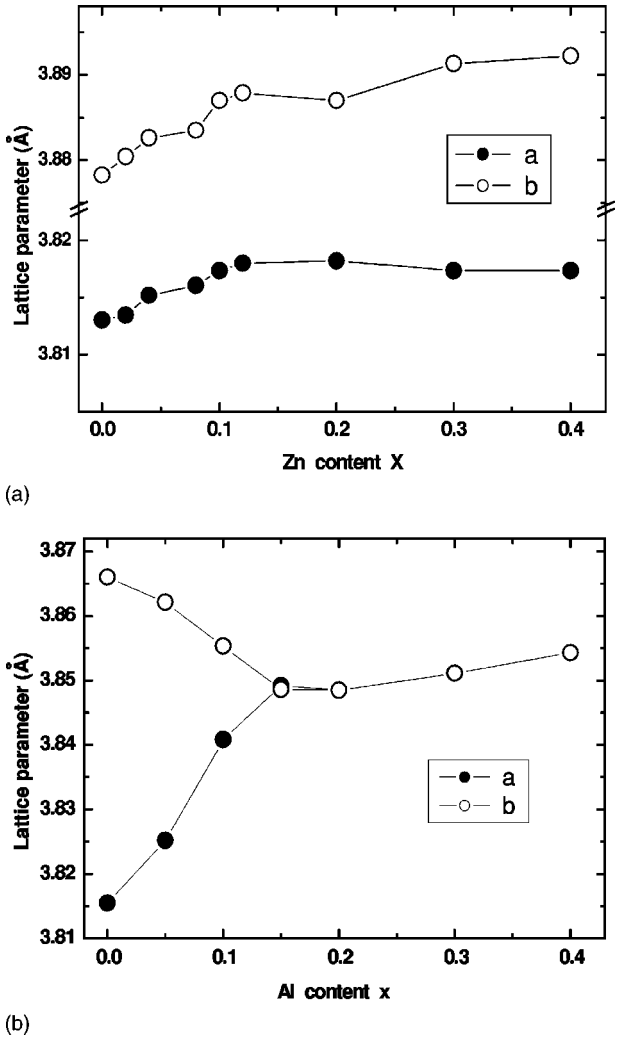

FIG. 1. (a) Lattice parameters as a function of Zn doping content x. O-T transition does not occur in the range of whole doping. (b) Lattice parameters as a function of Zn doping content x. O-T transition occurs near $x=0.15$.

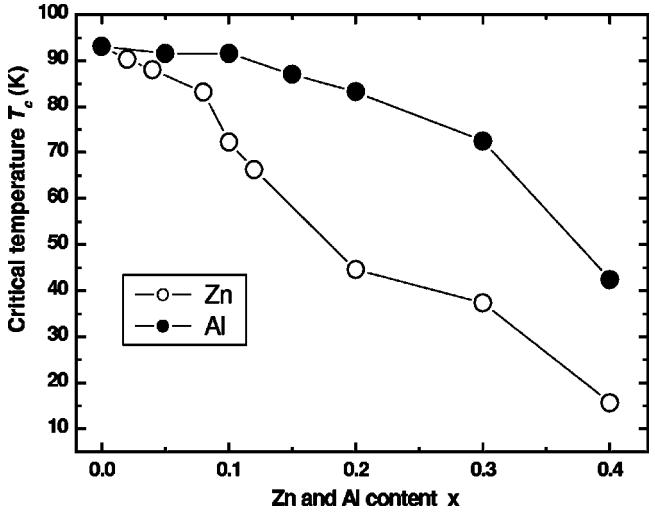

FIG. 2. Critical temperature T_c versus Zn and Al content x.

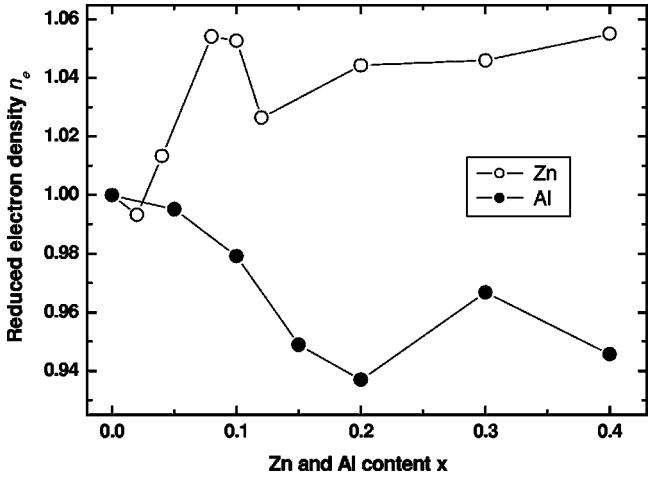

FIG. 3. The reduced electron density n_e as a function of Zn and Al content x.

B. Change of positron lifetime and local electron density

From Table I it can be seen that the short lifetime τ_1 varies in the range of 182–195 ps and the long lifetime τ_2 does 528–561 ps for Zn doping Y123 systems. While for Al doping, τ_1 varies from 195 to 206 ps and τ_2 from 549 to 602 ps. These results are typical characteristics in the ceramic samples.[31] According to the model of the two-state capture,[32,33] the process of positron annihilation is attributed to free-state and trapping-state annihilation in condensed matters. The positron lifetime is defined as the inverse of the annihilation rate. The short lifetime τ_1 reflects mainly the characteristics of free-state annihilation for the perfect crystal lattice, while the long lifetime τ_2 reveals mainly the process of positrons capture at imperfect regions, which may be divided into the bulk imperfects and microvoids. The former includes the cation deficiency, oxygen vacancy, twin boundary, dislocation, and so on. In general, the lifetime parameter τ_2 originates from these imperfects. The latter as microvoids denotes a longer lifetime than τ_2, sometimes one designates it as τ_3, generally $\tau_3 > 800$ ps,[20] this parameter is not recorded in the present experiment and would not be considered in the present work. Here τ_1 and τ_2 reveal the intrinsic characteristics of the samples. Hence, the relation between the annihilation rate λ and the local electron density n_e is defined as follows:

$$\lambda = \pi r_0^2 c n_e, \tag{1}$$

where r_0 is the classical electron radius and c is the light velocity. While $\lambda = 1/\tau_{\text{bulk}}$, and the bulk lifetime τ_{bulk} can be calculated from [11,34]

$$\frac{1}{\tau_{\text{bulk}}} = \frac{I_1}{\tau_1} + \frac{I_2}{\tau_2}. \tag{2}$$

Where I_1, the intensity of short lifetime, denotes the proportion of free-state annihilation to total annihilation events; I_2 denotes the corresponding proportion as the intensity of long lifetime and $I_2 = 1 - I_1$. Figure 3 shows the reduced electron density n_e varies with Zn and Al content x. For Zn doping, n_e decreases slightly as $x \leqslant 0.02$, then it increases rapidly to the maximum before $x = 0.1$, after an abrupt drop at $x = 0.12$, n_e gradually goes up to a high saturation value. On the whole, n_e increases with the increasing Zn content x. In contrast, the local electron density n_e decreases for Al doping. It decreases evidently until $x = 0.20$ and exhibits a fluctuation feature above $x = 0.2$. Significantly, both n_e display an abrupt change near the impurity phases appearing, namely, at $x = 0.12$ for Zn doping and $x = 0.20$ for Al doping, respectively. This characteristic reveals the intrinsic correlation between positron lifetime and impurity phases. On the other hand, this indicates the reliability of the present experimental results.

For the undoped Y123 systems, the relevant researches have proved that positron density distribution is not uniformity inside the materials. Because positrons prefer to annihilate in oxygen imperfection areas,[35,36] there is a high annihilation rate in the Cu-O chains.[11,34] According to the structural characteristic and charge distribution in $YBa_2Cu_3O_{7-\delta}$ systems, it is considered that the hole carriers originate from the Cu-O chains as a part of carrier reservoirs. The process is as follows: Once introduced into the Cu-O chains, every oxygen ion will attract two electrons for the requirement of the charge equilibrium. Meanwhile, two holes appear in the Cu-O chain region. On the whole, half of the holes are absorbed by Cu(1) ions, namely, Cu(1) changes from +1 into +2 valence; half of the remaining holes stay in the reservoir layer, and the rest (one fourth) of the holes transfer to the CuO_2 plane region. Therefore, the average valence state of Cu ion is generally +2.25 in the CuO_2 plane,[37] where the valence electron density is smaller than that in the Cu-O chain. For doped YBCO systems, once doped ions enter the Cu-O chains, oxygen imperfections will lessen, which drives a part of positrons transfer to the CuO_2 planes, the annihilation spectra will exhibit an increase in lifetime, i.e., the local electron density n_e should decrease as the increase of Al doping. On the contrary, while entering the CuO_2 planes, doped ions will attract positrons to annihilate in the CuO_2 planes, as Zn ions do. The Jean *et al.* calculation about the effect of Zn doping displays the same characteristics in the normal state.[11] Therefore, n_e should decrease likewise. However, the actual process is possibly much more

complicated, this is why the bivalence doped ions distinguish markedly from the trivalence ions in the influence on positron lifetimes: Al ions enter the Cu-O chains and drives incessantly positrons to the CuO_2 planes, whether the ions gather into clusters or not. But the case of Zn doping is not so simple, because the positrons are attracted into the CuO_2 planes and annihilated directly around the doped ions, the distribution of these ions will strongly influence the positron lifetimes. Single doped ions cannot create oxygen vacancies, so positrons annihilate simply in the CuO_2 planes. Once gathering into clusters, the doped ions can make the vacancies as imperfections, where positrons prefer to annihilate as above. Moreover, the doped ions show 0.25 valences lower than Cu; valence electrons lose less. Significantly, these ions possibly induce holes' escape from oxygen ions;[38,39] these two factors determine that the average density of valence electrons should be larger within clusters than in the CuO_2 planes. The calculation results of Jensen *et al.*[40] and Bharathi *et al.*[41] show that about 90% of positrons annihilate with the valence electrons, only about 10% of positrons annihilate with the electrons within the atomic kernel. As a result, once the doped ions enter the CuO_2 planes and form clusters, positrons prefer to annihilate within the clusters with higher density of valence electrons, naturally, n_e will show an increased trend. This conforms to the Jean *et al.* results, namely, at room temperature, the bulk lifetime τ_{bulk} exhibits a decreased trend with doping content x increases from 0 to 0.07.[11] In fact, the above conclusion is reasonable also to +3 valence ion clusters, in which there is only lower average density of valence electrons, if positrons annihilate within such clusters, n_e should decrease. But positrons do not prefer to annihilate within such ion clusters due to lack of oxygen vacancies. If doped ions enter Cu(1) and Cu(2) sites at the same time, n_e should be influenced by both the above two factors.

C. Simulated calculations for total defect and binding energy

In order to understand how the doped ions enter the different Cu sites, simulations were made in the present work. The calculations are based on the crystal lattice structures with energy minimization principle and formulated within the framework of the Born model, in which the effective pairwise potentials represent the interatomic forces in the following form:

$$\Phi_{ij} = \frac{Z_i Z_j e^2}{4\pi\varepsilon_0 r_{ij}} + A_{ij}\exp\left\{-\frac{r_{ij}}{\rho_{ij}}\right\} - \frac{C_{ij}}{r_{ij}^6}, \tag{3}$$

where Φ_{ij} is the effective potentials between ion i and ion j; Z_i and Z_j are ion valences; r_{ij} is the distance between ion i and ion j; A_{ij}, C_{ij}, and ρ_{ij} are the relative character constants. The first term is the long-range Coulomb interaction; the remaining terms represent the short-range interaction and the shielded revision.[26] Due to the demand of charge equilibrium, single doped ion cannot change copper-oxygen coordination, which may be carried out by the proper ion clusters in electric neutrality. The neutral clusters may show several structures, of which two kinds of typical shapes are illustrated in Fig. 4(a) in the CuO_2 planes for Zn doping and Fig. 4(b) in the Cu-O chain layers for Al doping. Tables II and III

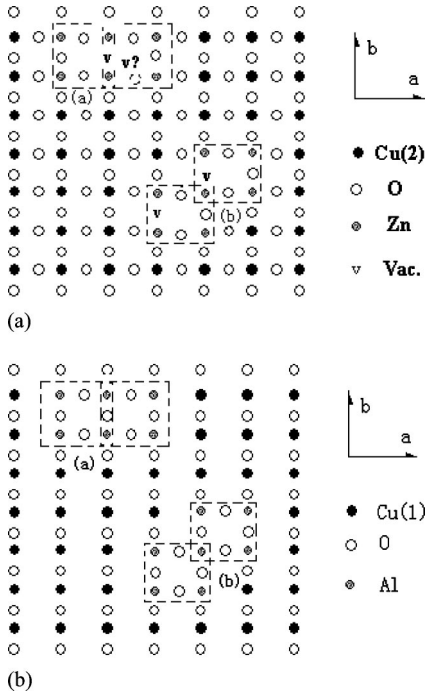

FIG. 4. (a) The doping Zn ions enter Cu(2) sites in the CuO_2 plane regions and gather into the ion clusters: (a) hexamer, (b) double square. (b) The doping Al ions enter Cu(1) sites in the Cu-O chain regions and gather into ion clusters: (a) hexamer, (b) double square.

list the calculated results of several clusters. For clusters, for example, a cluster of four Zn ions as tetramer is described as $\{4Zn^{2+} \rightarrow 4Cu^{2.25+} - O^{2-}\}$, the meaning is four Zn^{2+} ions substitution for four $Cu^{2.25+}$ ions, and then an O^{2-} ion will be squeezed out of the tetramer. It has the following binding energy E_{bind}:

$$E_{\text{bind}} = E_{b1}(4Zn^{2+} \rightarrow 4Cu^{2.25+} - O^{2-}) - 4E_{b2}(Zn^{2+} \rightarrow Cu^{2.25+}) + E_{b3}(O^{2-}), \tag{4}$$

where E_{b1}, E_{b2}, and E_{b3} are all represented by $E = \Sigma\Phi_{ij}$. E_{b1} is the total binding energy of a cluster, E_{b2} is the binding energy of a Zn^{2+} substitution for a $Cu^{2.25+}$ ion, and E_{b3} is the

TABLE II. The total defect energy of Zn^{2+}-oxygen vacancies and the average binding energy per ion in the CuO_2 planes, where E_{b1} (eV) is total defect binding energy in a cluster, and E_{maen} (eV/ion) is the average binding energy per doped ion.

Cluster structure	E_{b1} (eV)	E_{maen} (eV/ion)
Dimmer $\{2Zn^{2+} \rightarrow 2Cu^{2.25+}$ no $O^{2-}\}$	−31.15	−1.67
Tetramer $\{4Zn^{2+} \rightarrow 4Cu^{2.25+} - O^{2-}\}$ linear	−59.32	−1.49
Tetramer $\{4Zn^{2+} \rightarrow 4Cu^{2.25+} - O^{2-}\}$ square	−60.91	−1.64
Tetramer $\{4Zn^{2+} \rightarrow 4Cu^{2.25+} - O^{2-}\}$ zigzag	−59.03	−1.36
Hexamer $\{6Zn^{2+} \rightarrow 6Cu^{2.25+} - 2O^{2-}\}$	−97.26	−1.68
Hexamer $\{6Zn^{2+} \rightarrow 6Cu^{2.25+} - O^{2-}\}$	−108.55	−1.75
Double square $\{7Zn^{2+} \rightarrow 7Cu^{2.25+} - 2O^{2-}\}$	−122.97	−1.78

TABLE III. The total defect energy of Al^{3+}—interstitial oxygen and the average binding energy per ion in the Cu-O chains, where E_{b1} (eV) is total defect binding energy in a cluster, and E_{maen} (eV/ion) is the average binding energy per doped ion.

Cluster structure	E_{b1} (eV)	E_{maen} (eV/ion)
Dimmer $\{2Al^{3+} \rightarrow 2Cu^{2+} + O^{2-}\}$	−73.37	−2.73
Tetramer $\{4Al^{3+} \rightarrow 4Cu^{2+} + 2O^{2-}\}$ linear	−144.03	−2.25
Tetramer $\{4Al^{3+} \rightarrow 4Cu^{2+} + 2O^{2-}\}$ square	−145.94	−2.71
Tetramer $\{4Al^{3+} \rightarrow 4Cu^{2+} + 2O^{2-}\}$ zigzag	−143.18	−2.10
Hexamer $\{6Al^{3+} \rightarrow 6Cu^{2+} + 4O^{2-}\}$	−239.29	−2.85
Double square $\{7Al^{3+} \rightarrow 7Cu^{2+} + 4O^{2-}\}$	−265.41	−2.81

binding energy of a lost O^{2-} ion, while every doping ion has the average binding energy $E_{\mathrm{mean}} = E_{\mathrm{bind}}/4$. Other clusters may likewise be described and calculated. As is well known, the larger the average binding energy, the more stable the cluster combines. Consequently, the doped ions should prefer to form the cluster with the largest average binding energy. It can be concluded from the results listed in Tables II and III that the doped Al ions prefer to form hexamer clusters, while the doped Zn ions of double square clusters have the largest probability.

D. From dopant clusters to carrier localization

It is well known that for doped Y123 systems, Zn ions occupy Cu(2) sites. As a nonmagnetic ion, Zn doping not only destroys the antiferromagnetic order in the CuO_2 planes but also causes the change in electron structure around the doped Zn ions. As the above statements, the doped Zn ions make positrons prefer to annihilate in the CuO_2 planes, where the electron density is smaller than that in the Cu-O chains. While the Zn doping content is small, $x=0.02$, n_e should decrease, this feature is shown in Fig. 3. With the increase of Zn content, the ions gather into clusters and prefer to create oxygen vacancies, which can be confirmed from the relevant experiments that oxygen content decreases gradually.[10] These vacancies attract positrons to annihilate within the clusters with the higher density of valence electrons, thus n_e increases gradually. At the same time, the clusters suppress the superconductivity strongly. When $x \geqslant 0.12$, in terms of XRD results, impurity phases appear in the doped cuprates. In this case, it may be very complex that how Zn ions occupy different sites and where the positron would be annihilated. But Zn ions strongly suppress the superconductivity, namely, the T_c is depressed fast before $x=0.20$. Zn ions in impurity phases do not stay in the CuO_2 planes, thus the ability of depressing T_c becomes weakening as shown in Fig. 3. In a word, the clusters may significantly influence the positron annihilation characteristics. For example, the local electronic density n_e varies in complexity with the Zn doped content, which may get a satisfactory explanation from the clustering process. Without clusters, n_e should decrease monotonically, because Zn doping makes more positrons annihilating in the CuO_2 planes, where an increase in lifetime is observed as above. Obviously, PAT experiments support the clustering concept. In fact, this concept can be proved by the decrease of oxygen content with the increase of Zn doping ions,[10] because single Zn ion cannot drive out an oxygen ion from the crystal lattices. During the doping process, Zn ions substitute mainly for Cu(2) sites in the CuO_2 planes, where does occur the superconductivity, these doped ions make the change of electron structure and the carriers are strongly localized,[42,43] and therefore interfere the pairing and transportation of superconducting carriers, the superconductivity is suppressed more dramatically with the formation of Zn ion clusters.

In contrast to Zn doping, with increasing Al content x, n_e decreases monotonically. As +3 valence ion, Al easily enters Cu(1) site in the Cu-O chain[9] and requires more oxygen for coordination. When two Al ions form a small cluster, they will carry an extra oxygen ion into the Cu-O chains, where the oxygen vacancies decrease correspondingly, and a part of positrons shift from the Cu-O chains to the CuO_2 planes. An increase in lifetime is observed if positrons annihilate in the CuO_2 planes, thus the local electron density n_e decreases until $x=0.20$. At the same time, the doped Al ions slightly suppress the superconductivity. After the impurity phase appears for $x \geqslant 0.2$, n_e fluctuates markedly, perhaps because a part of Al ions enter the CuO_2 planes. Therefore, T_c is depressed more quickly (Fig. 3). Consequently, the change of local electron density n_e should reflect the intrinsic characteristics for Al doping YBCO systems. Significantly, it is Al ion clusters that bring the extra oxygen ions into the Cu-O chains, while single Al ion itself cannot do these. In terms of the calculated results and the valence analysis as above, Al ions should gather into clusters, which is proved by the fact that the increase of oxygen content with Al ions increasing.[10] Whether the doped Al ions form clusters or not, positron lifetimes are not influenced probably, but the electronic structure of the Cu-O chains are influenced by the clusters. Therefore, we emphasize the Al doping ion clusters. Al doping may influence the superconductivity in the following way: When two Al ions as the smallest cluster carry an oxygen ion into the Cu-O chains, due to the charge equilibrium between Al and oxygen ions, superabundant holes cannot be generated, the holes as carriers decrease gradually with increasing Al content. Along with the formation of larger clusters, hole carriers are restricted or localized in the Cu-O chains. Namely, there are not enough holes to be transferred to the CuO_2 planes, which weakens the function of carrier reservoir and suppresses the superconductivity. Therefore, Al doping affects indirectly the pairing and transportation of carriers. Accordingly, Al doping depresses T_c weakly than Zn doping in YBCO systems.

IV. CONCLUSIONS

The high-T_c cuprates $YBa_2Cu_{3-x}(Zn,Al)_xO_{7-\delta}$ ($x=0.0-0.4$) have been systemically studied by the positron annihilation technique, x-ray diffraction, and the simulated calculation. The results indicate that both doping Zn and Al ions would combine into the different clusters of two, four, six, or seven ions. These ions prefer to form the cluster of

seven ions as double square and six ions as hexamer, respectively. The variation of local electron density n_e with Zn content x can be explained from the clustering process. In both cases, n_e display an abrupt change near the appearance of impurity phases in the Zn and Al doping systems. This characteristic reveals the intrinsic correlation between positron lifetime and the impurity phases. The doping Zn ions occupy Cu(2) sites in the CuO_2 planes, where the superconductivity occurs. These ions make the change of electron structure and the carriers are strongly localized, so they interfere the pairing and transportation of carriers and suppress the superconductivity with the formation of Zn clusters. While the doped Al ions enter Cu(1) sites in the Cu-O chains, which induces the localization of hole carriers and weakens the function of the Cu-O chains as carrier reservoir by clusters. Hence, the hole carriers cannot easily transfer to the CuO_2 planes. The pairing and transportation of carriers are affected indirectly, and the superconductivity is suppressed weaker than the case of Zn doping.

ACKNOWLEDGMENTS

This work is supported by the National Foundation of Natural Science of People's Republic of China (No. 10274049), the Dawn Project (No. 03SG35), the Science and Technology Development Foundation of the Education Committee of Shanghai Municipality (No. 02AK42), and the Shanghai Leading Academic Discipline Program.

*Corresponding author: Email address: jczhang@mail.shu.edu.cn

[1] D. K. Morr and A. V. Balatsky, Phys. Rev. Lett. **90**, 067005 (2003).
[2] S. Q. Guo, F. L. Wang, Y. L. Zhou, B. R. Zhao, and J. Gao, Chinese Phys. **11**, 379 (2002).
[3] R. Lortz, C. Meingast, and A. I. Rykov, Phys. Rev. Lett. **91**, 207001 (2003).
[4] J. Axnas, W. Holm, Y. Eltsew, and O. Rapp, Phys. Rev. B **53**, R3003 (1996).
[5] B. Nachumi, A. Keren, K. Kojima, M. Larkin, G. M. Luke, J. Merrin, O. Tchernyshov, Y. J. Uemura, N. Ichikawa, M. Goto, and S. Uchida, Phys. Rev. Lett. **77**, 5421 (1996).
[6] Y. K. Kuo, C. W. Schneider, M. J. Skove, M. V. Nevitt, G. X. Tessema, and J. J. McGee, Phys. Rev. B **56**, 6201 (1997).
[7] R. S. Horland and T. H. Geballe, Phys. Rev. B **39**, 9017 (1989).
[8] D. M. Ginsberg, *Physical Properties of High Temperature Superconductors II* (World Scientific, Singapore, 1990), p. 543.
[9] L. Hoffmann, A. A. Manuel, M. Peter, E. Walker, M. Gauthier, A. Shukla, B. Barbiellini, S. Massidda, Gh. Adam, W. N. Hardy, and R. X. Liang, Phys. Rev. Lett. **71**, 4047 (1993).
[10] J. M. Tarascon, P. Barboux, P. F. Miceli, L. H. Greene, G. W. Hull, M. Eibschutz, and S. A. Sunshine, Phys. Rev. B **37**(13), 7458 (1988).
[11] Y. C. Jean, C. S. Sunder, A. Bharathi, J. Kyle, H. Nakanishi, P. K. Tseng, P. H. Hor, R. L. Meng, Z. J. Huang, C. W. Chu, Z. Z. Wang, P. E. A. Turchi, R. H. Howell, A. L. Wachs, and M. J. Fluss, Phys. Rev. Lett. **64**, 1593 (1990).
[12] H. Takagi, Physica C **341–348**, 3 (2000).
[13] W. Guo and R. S. Han, Chin. Phys. Lett. **18**, 582 (2001).
[14] Allan Hugh MacDonald, Nature (London) **414**, 409 (2001).
[15] M. Capone, M. Fabrizio, C. Castellani, and E. Tosatti, Science **296**, 2364 (2002).
[16] K. Saarinen, J. Nissila, H. Kauppinen, M. Hakala, M. J. Puska, P. Hautojarvi, and C. Corbel, Phys. Rev. Lett. **82**, 1883 (1999).
[17] C. Nagel, K. Ratzke, E. Schmidtke, F. Faupel, and W. Ulfert, Phys. Rev. B **60**, 9212 (1999).
[18] T. E. M. Staab, M. Haugk, Th. Frauenheim, and H. S. Leipner, Phys. Rev. Lett. **83**, 5519 (1999).
[19] A. Somoza, A. Dupasquier, I. J. Polmear, P. Folegati, and R. Ferragut, Phys. Rev. B **61**, 14454 (2000).
[20] T. Banerjee, R. N. Viswanath, D. Kanjilal, R. Kumar, and S. Ramasamy, Solid State Commun. **114**, 655 (2000).
[21] Udayan De, D. Sanyal, S. Chaudhuri, P. M. G. Nambissan, Th. Wolf, and H. Wuhl, Phys. Rev. B **62**, 14519 (2000).
[22] Y. C. Jean, J. Kyle, H. Nakanishi, and P. E. A. Turchi, Phys. Rev. Lett. **60**, 1069 (1988).
[23] E. C. von Stetten, S. Berko, X. S. Li, and R. R. Lee, Phys. Rev. Lett. **60**, 2198 (1988).
[24] J. C. Zhang, F. Q. Liu, G. S. Cheng, J. X. Shang, J. Z. Liu, S. X. Cao, and Z. X. Liu, Phys. Lett. A **201**, 70 (1995).
[25] J. C. Zhang, L. H. Liu, C. Dong, J. Q. Li, H. Chen, X. G. Li, and G. S. Cheng, Phys. Rev. B **65**, 054513 (2002).
[26] M. S. Islam and C. Ananthamohan, Phys. Rev. B **44**, 9492 (1991).
[27] J. F. Bringley, T. M. Chen, B. A. Averill, K. M. Wong, and S. J. Poon, Phys. Rev. B **38**, 2432 (1988).
[28] J. M. Tarascon, L. H. Greene, P. Barboux, W. R. McKinnon, G. W. Hull, T. P. Orlando, K. A. Delin, S. Foner, and E. J. McNiff, Jr., Phys. Rev. B **36**, 8393 (1987).
[29] G. Xiao, M. Z. Cieplak, and C. L. Chien, Phys. Rev. B **42**, 240 (1990).
[30] N. Bulut, D. Hone, D. J. Scalapino, and E. Y. Loh, Phys. Rev. Lett. **62**, 2192 (1989).
[31] R. P. Gupta and M. Gupta, Physica C **305**, 179 (1998).
[32] W. Brandt and J. Reinheimer, Phys. Lett. **35A**, 109 (1971).
[33] W. Brandt, *Positron Annihilation* (Academic Press, New York, 1967), p. 155.
[34] S. Ishibashi, R. Yamamoto, M. Doyama, and T. Matsumoto, J. Phys.: Condens. Matter **3**, 9169 (1991).
[35] J. D. Jorgensen, Phys. Today **44**, 34 (1991).
[36] B. Chakraborty, Phys. Rev. B **39**, 215 (1989).
[37] H. B. Zhang and H. Sato, Phys. Rev. Lett. **70**, 1697 (1993).
[38] P. C. Li, H. S. Yang, Z. Q. Li, Y. S. Chai, and L. Z. Cao, Chinese Phys. **11**, 282 (2002).
[39] H. Haghighi, J. H. Kaiser, S. Rayner, R. N. West, and M. J. Fluss, J. Phys.: Condens. Matter **2**, 1911 (1990).
[40] K. O. Jensen, R. M. Nieminen, and M. J. Puska, J. Phys.: Condens. Matter **1**, 3727 (1989).
[41] A. Bharathi, C. S. Sundar, and Y. Hariharan, J. Phys.: Condens. Matter **1**, 1467 (1989).

[42] S. T. Wei, F. L. Liu, S. X. Cao, and J. C. Zhang, Mater. Lett. **35**, 27015 (1998).

[43] J. C. Zhang, Y. J. Cui, D. M. Deng, H. M. Xing, Z. P. Chen, X. G. Li, and G. S. Cheng, Phys. Lett. A **26**, 452 (1999).